J Membrane Biol (2013) 246:769–781
DOI 10.1007/s00232-013-9547-6

Inactivation of *Pseudomonas putida* by Pulsed Electric Field Treatment: A Study on the Correlation of Treatment Parameters and Inactivation Efficiency in the Short-Pulse Range

Wolfgang Frey · Christian Gusbeth · Thomas Schwartz

Received: 19 December 2012 / Accepted: 17 April 2013 / Published online: 10 May 2013

Abstract An important issue for an economic application of the pulsed electric field treatment for bacterial decontamination of wastewater is the specific treatment energy needed for effective reduction of bacterial populations. The present experimental study performed in a field amplitude range of $40 > E > 200$ kV/cm and for a suspension conductivity of $0.01 = \kappa_e > 0.2$ S/m focusses on the application of short pulses, 25 ns $> T >$ 10 µs, of rectangular, bipolar and exponential shape and was made on *Pseudomonas putida*, which is a typical and widespread wastewater microorganism. The comparison of inactivation results with calculations of the temporal and azimuthal membrane charging dynamics using the model of Pauly and Schwan revealed that for efficient inactivation, membrane segments at the cell equator have to be charged quickly and to a sufficiently high value, on the order of 0.5 V. After fulfilling this basic condition by an appropriate choice of pulse field strength and duration, the log rate of inactivation for a given suspension conductivity of 0.2 S/m was found to be independent of the duration of individual pulses for constant treatment energy expenditure. Moreover, experimental results suggest that even pulse shape plays a minor role in inactivation efficiency. The variation of the suspension conductivity resulted in comparable inactivation performance of identical pulse parameters if the product of pulse duration and number of pulses was the same, i.e., required treatment energy can be linearly downscaled for lower conductivities, provided that pulse amplitude and duration are selected for entire membrane surface permeabilization.

Keywords Inactivation of bacteria · Pulsed electric field treatment · PEF-inactivation · Wastewater disinfection · Electroporation · Plasma membrane charging

W. Frey (✉) · C. Gusbeth
Institute for Pulsed Power and Microwave Technology, Karlsruhe Institute of Technology, Hermann-von-Helmholtz-Platz 1, Eggenstein-Leopoldshafen 76344, Germany
e-mail: wolfgang.frey@kit.edu

T. Schwartz
Institute of Functional Interfaces, Karlsruhe Institute of Technology, Hermann-von-Helmholtz-Platz 1, Eggenstein-Leopoldshafen 76344, Germany

Introduction

Pulsed electric field (PEF) treatment of wastewater was demonstrated to be an advantageous alternative to conventional disinfection methods. Chlorination or ozonization produces unwanted toxic by-products originating from chemical reactions with organic substances in wastewater (Galapate et al. 2001; Sohn et al. 2004). UV disinfection efficiency is reduced for high particle densities in wastewater because of the low penetration depth of UV light and dark repair abilities of bacteria (Jungfer et al. 2007). Especially for highly contaminated clinical wastewater, PEF disinfection was proven to cause no adverse effects, such as genotoxicity, phenotypic changes, or adaption of the bacteria to repeated PEF treatment (Gusbeth et al. 2009). Moreover, PEF treatment preserves nuclease activity, providing enzymatic degradation of DNA (Rieder et al. 2008). This can considerably reduce the spread of resistance plasmids originating from antibiotic-resistant bacteria in clinical wastewater. Despite all its advantages, PEF disinfection has to compete with conventional techniques from an economic point of view (Poyatos et al. 2011). This demands optimum treatment parameters, resulting in a highly energy efficient method. The work we present here

focuses on the influence of various PEF treatment parameters on the disinfection performance of this technique.

Bacterial inactivation by PEF treatment is based on the permeabilization of the plasma membrane of the microorganisms caused by an electric field across the membrane, which is higher than the field resulting from the cell's resting potential. To increase the membrane field, the cell membrane is charged by an external PEF applied to the cell suspension. At sufficiently elevated transmembrane voltage values, the membrane's phospholipid molecules rearrange into an energetically more favorable configuration by forming hydrophilic pores (see Neumann et al. 1989; Teissié et al. 2005; Tsong 1990; Weaver and Chizmadzhev 1996; Zimmermann et al. 1974). Electroporation—commonly agreed to be the main reason for membrane permeabilization—enables intracellular liquids to pass the membrane. This loss of cytoplasm constrains cell function and finally causes cell death.

The transmembrane voltage values for effective membrane permeabilization provided in the literature depend on the duration of the electric field pulse and range from 0.2 to 1.6 V (Weaver et al. 2012). For short pulses, on the order of several 10 ns, the membrane voltage can exceed values of 1 V (Frey et al. 2006). For longer pulses (on the microsecond timescale), a membrane voltage value of 0.3–0.5 V experimentally (Flickinger et al. 2010; Gabriel and Teissié 1997; Hibino et al. 1993; Teissié and Rols 1993) and theoretically (Neu and Krassowska 1999) was found to be sufficient for onset of membrane permeabilization. Charging of a nonconductive dielectric shell, representing the membrane of spherical cells (diameter 2a) by an external electric field E, results in a cosine azimuthal distribution of the transmembrane voltage V_m (Kotnik et al. 1998; Pauly and Schwan 1959):

$$V_m(\theta,t) = 1.5 \cdot E_a \cos(\theta) \cdot (1 - \exp(-t/\tau_C));\ \tau_C = aC_m(1/\kappa_i + 1/2\kappa_e) \quad (1)$$

C_m designates the membrane capacity per area and κ_i and κ_e intracellular and external medium conductivity. Membrane voltage exponentially rises with a time constant of τ_c in response to a step-function field pulse applied to the cell suspension. Generally, large values of V_m are achieved first at membrane regions facing the electrodes (cell poles, $\theta = 0°$, 180°) and low values at the cell equator region ($\theta = 90°$, 270°). In consequence, the required external field amplitude for permeabilizing the equatorial region of the cell membrane is high compared to the required values for cell pole permeabilization. Because of the lack of criteria about which fraction of the cell surface has to be charged to at least 0.5 V for efficient PEF inactivation, pulse parameters, i.e., field amplitude and duration, cannot be calculated a priori. Despite considerable progress made in modeling bacterial inactivation (Huang et al. 2012; Saldana et al. 2011), the temporal evolution of pore size and pore density, which follows on membrane charging, and its influence on inactivation efficiency can only be predicted theoretically in first approximation for simplified membrane models, i.e., lipid bilayers, so far. Even nowadays, optimum treatment parameters for PEF inactivation of bacteria still have to be determined experimentally.

In the early 1960s, Sale and Hamilton first performed comprehensive experimental studies on bacterial inactivation by rectangular PEFs (Hamilton and Sale 1967; Sale and Hamilton 1967). They had already concluded from their work that plasma membrane permeabilization causes cell death by lysis (Sale and Hamilton 1968). Furthermore, they found that the inactivation rate directly scales with the applied electric field strength and the treatment time, i.e., the product of the number of pulses and the pulse duration. A decade later, basic work on the mechanisms of field-induced membrane permeabilization was performed by Hülsheger and Niemann. Exponential decaying pulses were used in inactivation experiments. For a specific treatment energy of 125 J/ml, an inactivation of 3.5 log on *Escherichia coli* was obtained (Hülsheger and Niemann 1980; Hülsheger et al. 1981). Hülsheger confirmed a linear relation between field strength and inactivation rate after exceeding a critical value of the applied electric field strength. At the same time, Sakarauchi and Kondo (1980) found a direct correlation between applied energy and inactivation rate.

Starting in the early 1990s, many publications focused on experimental studies on various bacteria/suspension configurations, predominantly at the background of non-thermal food preservation. There is a general consensus in the literature that the major parameters that affect inactivation efficiency are field amplitude E, pulse shape, pulse duration T, and overall treatment time $N{\cdot}T$ (Abram et al. 2003; Álvarez et al. 2003a; Castro et al. 1993; Wouters et al. 2001a), with N denoting the number of pulses delivered to a finite volume. Specific treatment energy W, which for a given suspension conductivity κ_e and uniform field distribution in the treatment chamber, calculates to

$$W = \kappa_e N \int_T E^2(t)\mathrm{d}t, \quad (2)$$

which has also been identified to be a determining treatment parameter (Heinz et al. 2007; Schoenbach et al. 2000, 2009). Other important factors not related to the electrical parameters are media temperature (Saldana et al. 2011; Toepfl et al. 2007), treated bacteria species (Wouters et al. 2001a), growth phase (Wouters et al. 2001b), and media composition (Ait-Ouazzou et al. 2013) and properties, i.e., pH (Aronsson et al. 2001; Garcia et al. 2003; for a

summary, see Saulis 2010; Sobrino-López and Martín-Belloso 2010). Because of different treatment conditions and a partially incomplete description of experimental conditions, a general application-relevant parameter recommendation for best-efficiency PEF inactivation cannot be adopted from literature; rather, it must be verified individually by experiments.

The following study is restricted to field pulses of 10 µs and shorter. At this timescale, breakdown probability in uniform field treatment chambers as a result of unavoidable gas bubbles was found to be low. In addition, electrode erosion by iron release from stainless steel electrodes, preferentially used in industrial-size and continuously operating treatment facilities (Rieder et al. 2008), was proven to be lower for microsecond-length pulses compared to longer pulses (Toepfl et al. 2007).

Materials and Methods

Cell Culture and Preparation

The Gram-negative bacterium *Pseudomonas putida* (German type collection strain DSM 291) was cultivated on R2A agar (Difco) commonly used for heterotrophic bacteria (Reasoner and Geldreich 1985). Single colonies were suspended in 10 ml of a 1:4 diluted brain–heart infusion (Merck) for overnight incubation at 30 °C. A volume of 40 ml of brain–heart infusion (1:4) was inoculated with an aliquot of the overnight culture and incubated for at least 2 h at 30 °C. Bacteria were removed from culture in early stationary growth phase and immediately prepared for PEF treatment.

Because bacteria in environments like wastewater have to deal with unfavorable growth conditions in addition to diverse stresses, bacteria that reached the early stationary growth phase were used to imitate this environment (Nystrom 2004). During the transition from exponential growth to the stationary phase, growth becomes unbalanced, i.e., the synthesis of different macromolecules and cell constituents does not slow down synchronically. Thus, the early stationary phase is an operational definition and does not describe a specific and fixed physiological state or response of the bacteria. In consequence, this growth phase mimics the growth conditions in natural aquatic habitats, e.g., wastewater.

Just before PEF treatment, the medium was removed by centrifugation at 5,000 rpm for 5 min. The resulting bacteria pellet was washed with 15 ml EP buffer (1.25 mM Na-phosphate, 16.25 mM NaCl, pH 7.5) exhibiting a conductivity of 0.2 S/m. Conductivity was controlled at room temperature, 22 °C, by a handheld conductivity and temperature meter (CLM 381; Endress + Hauser). For measurement, temperature compensation was disabled. The washed pellet was finally suspended in EP buffer to reach an optical density at 600 nm of 0.6–0.8, representing a cell density of 10^7–10^8 cells/ml for subsequent PEF treatment.

Experimental Setup and Procedure

Electroporation cuvettes (BTX Instrument) with aluminum electrodes at a rated electrode distance of 2 mm and a volume of 400 µl were used in all experiments as treatment chambers. The scattering of the electrode distance of a sample of 30 cuvettes was measured by gauge blocks and determined to be ±0.1 mm in maximum. The cuvettes were connected to the pulse generator by copper–beryllium spring contact strips soldered onto 10-mm-wide and 1.5-mm-thick brass conductors, providing a low-inductance and low-resistance connection.

Rectangular pulses up to a pulse amplitude of 25 kV corresponding to a field strength of 12.5 MV/m were generated by a transmission line pulse generator (Fig. 1, right). Conventional 50 Ω coaxial cables (RG 213; Belden) were charged up to 50 kV via a charging resistor, $R_C = 100$ MΩ, and switched onto the load by a gas insulated pressurized spark gap. The resulting output pulse exhibits a voltage amplitude of 25 kV at a matched load of 50 Ω. The pulse duration is adjusted by varying the length of the transmission line cable. For our experiments, the cable length was varied between 10 and 1,000 m, which corresponded to a pulse duration ranging from 100 ns to 10 µs. The output line of the generator was 10 m long.

In order to minimize switch inductance, which affects the pulse rise time, SF_6 at a pressure of up to 200 kPa was used as insulating gas between the electrodes of the spark gap. The 10–90 % pulse rise time of the transmission line generator was $t_R = 16$ ns.

The spark gap was operated in the self-breakdown mode. Because of a preionization of the gap volume by an auxiliary corona discharge, accomplished by a needle-type electrode mounted in close vicinity to the ground electrode and connected to ground potential, the maximum pulse-to-pulse deviation of the voltage amplitude from the mean value was less than 5 % (Frey et al. 2009).

Pulses of 25 ns exhibiting a maximum field strength of 200 kV/cm were generated according to the Blumlein principle. To provide a generator impedance of 50 Ω, two 2.5-m-long coaxial cables (RG 213) were connected in parallel and charged to 40 kV (Fig. 1, middle). The pulse was released by the ignition of a SF_6 insulated pressurized spark gap. The pulse rise time was $T_R = 4.2$ ns.

Bipolar pulses were generated by a bidirectional pulse forming a line (Fig. 1, right) (Smith 2002). The cable lengths for 600 and 1,200 ns bipolar pulses providing a polarity change in the middle of the pulse were 60 and

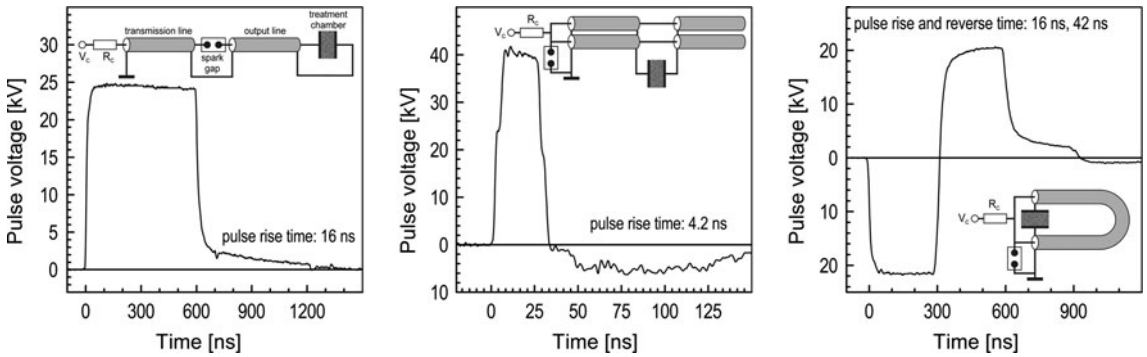

Fig. 1 Typical output pulse of the cable pulse generators used for the experiments. Transmission line generator (*left*), Blumlein generator (*middle*), and bipolar pulse generator (*right*)

120 m, respectively. For switching, a SF_6 insulated pressurized and corona-preionized spark gap operating in the self-breakdown mode was used as described above.

Exponential pulses were generated by discharging a capacitor bank onto the cuvette. For providing a slow decaying pulse, four capacitors (type 715C-Z; Sprague, Vishay Electronic) with a nominal capacitance of 3.3 nF were connected in parallel. For generating a shorter exponential pulse exhibiting equal energy content, the same four capacitors were used in a series-parallel connection (Fig. 2, right). The output voltage amplitude was adjusted to 16 kV for the slow decaying setup and to 32 kV for the series-parallel arrangement. The measured discharge time constants were 230 and 860 ns, respectively.

All types of pulse generator were charged by a 50 kV/10 mA power supply (type R50B; Hipotronics). Measurement data were acquired by a 500 MHz oscilloscope (TDS 640A; Tektronix). The voltage was measured by a calibrated Tektronix probe (P6015). The rise time of the acquisition system, i.e., the probe connected to the TDS 640A, was better than $t_R = 2$ ns. (For calibration details, see Eing et al. 2009.) The current waveform of exponential pulses was measured by a Pearson current monitor (model 410; Pearson Electronics), which was inserted into the ground lead of the load. Deviating from energy calculation used for square type pulses (Eq. 2) in cases of exponential pulses, the energy was calculated by integrating the product cuvette voltage times current over time.

For evaluation of the pulse, amplitude every pulse applied to the cuvettes during PEF treatment was acquired and stored digitally. Afterward, in case of square pulses, the amplitude of each pulse was evaluated as an average of digitized points between 10 and 90 % of the pulse duration. In case of exponential pulses, the pulse maximum was determined. The decrease of pulse amplitude as a result of conductivity increase was obvious during the first couple of pulses but was less than 10 % in the course of a cuvette treatment. For considering pulse-to-pulse variations, the pulse amplitude value characterizing the treatment of a cuvette was determined by averaging all single-pulse amplitude values. The electric field values given for the experiments discussed here are the average pulse amplitude values divided by the rated cuvette electrode distance and represent the evaluated average values of each treatment with an accuracy of ±5 kV/cm. In the following, typical measured pulse waveforms are displayed in combination with inactivation results for better traceability and understanding of various conditions.

During pulse treatment of the bacterial suspension, the time between two pulses was 2 s. One experiment typically consisted of a sequence of 10–15 cuvettes treated successively. A sham control was treated and analyzed for cell density for each experiment. The cuvettes were filled just

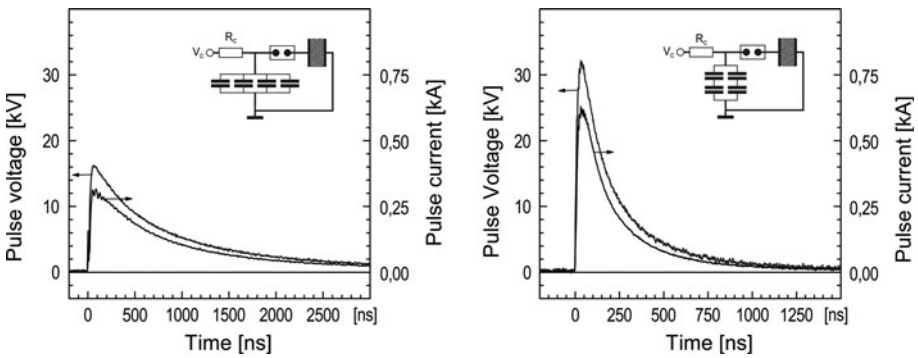

Fig. 2 Pulse generator setup for the generation of exponential decaying pulses of identical energy content but different decay times and amplitude. For accomplishing pulses of identical energy content, each capacitor was charged to the same value

before pulse treatment. To avoid a nonuniform field distribution in the suspension volume, in particular in the upper electrode region, the cuvettes were carefully filled to the upper edge of the electrodes with bacterial suspension and then coated with 20 µl of paraffin oil (high viscosity, No. 8904.1; Roth). Besides providing uniform field in the entire bacterial suspension volume to be treated, this measure also prevented surface flashover along the surface of the bacterial suspension. Before the experiments, this method of coating the suspension by paraffin oil was demonstrated to have no influence on bacterial viability. Immediately after pulse treatment of the last cuvette of the series, the determination of the inactivation rate was started. To exclude temperature effects on inactivation, the cuvette containing the bacteria suspension to be treated was immersed into 100 ml of transformer oil (Shell Diala DX) for cooling during PEF treatment. For an extreme treatment condition, the maximum temperature rise after a PEF treatment at 800 J/ml was measured to be 7 °C.

Determination of Inactivation Rates

Volumes of 400 µl of bacteria suspension in EP buffer were filled in the electroporation cuvettes for PEF treatment. The bacterial densities of untreated and treated samples were calculated via the pour plate method with R2A agar. Serial dilutions from the bacteria suspensions ranging from 10^{-1} to 10^{-7} were made, and aliquots of the dilutions were used for determination of the colony-forming units (CFU). The agar plates were incubated at 30 °C for 5 days. All experiments were performed in triplicate and repeated three times unless otherwise stated. The averages of CFU of the different dilutions were calculated as CFU/ml. Only counts between 25 and 300 CFU per plate were considered for evaluation. The inactivation rates were expressed as $\log_{10}$ number differences between the untreated control and treated bacterial suspensions. The error bars in the figures denote the standard deviation σ of the log rate of inactivation.

Results

This study focuses on the assessment of energy-efficient PEF treatment parameters in the short-pulse regime for inactivation of bacteria in aqueous suspension. *Pseudomonas putida* was used as model organism, which is known to be present and adapted in diverse aquatic compartments, e.g., wastewater, drinking water, and industrial-process water. Parameters under investigation were PEF amplitude E, pulse duration T, number of pulses N, energy per pulse W_p, energy per treated volume W, pulse shape, rectangular (unipolar and bipolar), and exponential decaying and extracellular medium conductivity κ_e at a constant medium temperature.

To test whether and to what extend membrane charging dynamics analyzed by a simplified model can be correlated to bacterial inactivation performance and whether it can be used for identifying treatment conditions for high inactivation efficiency, a spherical dielectric shell model was used to mimic the Gram-negative bacteria's cell membrane, which in reality is much more complex (Huang et al. 2008; Silhavy et al. 2010). To approximate the elliptical shape of *P. putida,* the diameter of spherical cells in the model was chosen to be in between the dimensions of major and minor axis. Furthermore, for simplicity, the field pulse was assumed to rise instantaneously (step function) for calculation. In consequence, the calculated time for reaching a membrane voltage value of 0.5 V has to be prolonged in maximum by the rise time of the pulses used in the experiments, i.e., $T_R = 16$ and 4.2 ns, respectively. This additional delay to the calculated values is significantly shorter than the pulse rise time in case the membrane voltage slowly—on a timescale of a 100 ns—approaches 0.5 V, e.g., close to the cell equator (cf. Fig. 5), and in case of high field amplitudes, $E \geq 80$ kV/cm, at the cell pole region, where 0.5 V is achieved during the first couple of nanoseconds. For these reasons, values for the time delay to reach 0.5 V in the following are discussed only to an accuracy of 10 ns. On the basis of the above-described approximations, we must point out that the following calculation results have to be regarded as a first-order approximation of membrane charging dynamics.

For the first orientation of short-pulse inactivation performance, experiments were started by applying an electric field strength of $E = 100$ kV/cm and a pulse duration of $T = 600$ ns. Here, the pulse duration exceeds the membrane-charging constant $\tau_c = 42$ ns, calculated for a spherical cell, $a = 1$ µm, suspension conductivity of $\kappa_e = 0.2$ S/m, cytoplasmic conductivity of $\kappa_i = 0.44$ S/m (Hoelzel 1999; Kotnik et al. 1998), and $C_m = 0.88$ µF/cm^2 (Kotnik et al. 1998; Vasilkoski et al. 2006) according to Eq. (1), providing membrane charging to a value of $V_m = 0.5$ V, required for the onset of membrane permeabilization, within less than 100 ns at the entire cell surface (cf. Fig. 5).

The energy delivered to the bacterial suspension was varied by increasing the number of 600 ns pulses. Ten pulses at 100 kV/cm represent a treatment energy of $W = 120$ J/ml. This experiment revealed that the log rate of inactivation does not increase linearly with expended treatment energy. Moreover, the inactivation rate saturates at 6 log (Fig. 3). It has to be pointed out that the suspension temperature rise during the treatment energy variation was less than 7 °C above room temperature. The results reflect bacterial inactivation purely as a result of the impact of the

PEF and was not promoted by electrically induced thermal heating. In case of not allowing the heat to equilibrate across the aluminum electrodes into the transformer oil reservoir surrounding the treatment cuvette, a treatment energy of $W = 800$ J/ml coupled electrically into the suspension would cause an adiabatic temperature rise of $\Delta T = 191$ K. In reality, as a result of heat dissipation, the suspension temperature in this case is far lower but still can temporarily elevate to values higher than 60 °C, which can considerably influence bacterial inactivation.

Measurements on the influence of the pulse duration were made at a constant field strength amplitude of 40 kV/cm. Successively, the pulse duration was set to 10, 5, 2, 1 µs, 600, 200, and 100 ns (Fig. 4, right). Treatment energy was adjusted to 120 J/ml by appropriately increasing the number of pulses according to Eq. (2). The inactivation rate was higher than 3 log for pulses longer than 600 ns (Fig. 4, left). For shorter pulses exhibiting a pulse duration of $T = 200$ and 100 ns, the inactivation rate obtained from three independent experiments decreased to 2.9 and 2.1 log on average. This can be explained by insufficient membrane charging at 40 kV/cm in case of applying a pulse duration of 200 ns and shorter.

The calculation of the temporal and azimuthal evolution of the membrane voltage according to Eq. (1) applying the parameters given above reveals that toroidal surface segments, which are located at the equator of the cell (cf. pictogram in Fig. 5, middle), are charged considerably more slowly than segments at the cell pole (Fig. 5, left). At an external field strength of $E = 40$ kV/cm, the membrane voltage across equatorial segments ($\theta = 85°$) reaches $V_m = 0.5$ V later than 100 ns (Fig. 5, left), whereas membrane segments at the cell pole ($5° < \theta < 35°$) are charged considerably faster—within about 10 ns to membrane voltage values above $V_m > 0.5$ V.

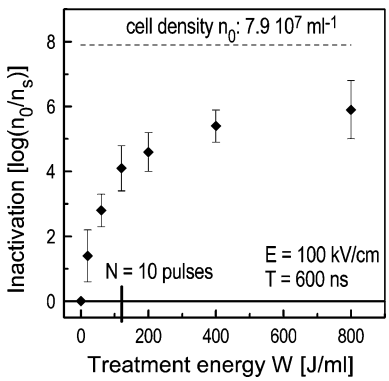

Fig. 3 PEF treatment of *P. putida* with 600 ns, 100 kV/cm square pulses at a conductivity of the extracellular medium of $\kappa_e = 0.2$ S/m. The inactivation rate saturates at 6 log. The initial cell density was 2 orders of magnitude higher

Both equatorial membrane segments represent 17.4 % of the total surface of a spherical cell. The decrease of inactivation efficiency for $T \leq 200$ ns (Fig. 4, left) suggests either insufficient membrane charging for effective membrane permeabilization or that the time period from reaching $V_m = 0.5$ V to the end of the pulse is too short for initiating sufficient inactivation-relevant membrane permeabilization at 40 kV/cm. The latter appears to be most probable because theoretical work has revealed that the membrane voltage required for the onset of formation of large pores is $V_m = 0.5$ V (Neu and Krassowska 1999). Furthermore, experimental work revealed that membrane permeabilization can already be detected when a membrane voltage value of $V_m = 0.3$ V has been exceeded (Flickinger et al. 2010; Teissié and Rols 1993). The results displayed in Fig. 4 in comparison to the calculated time course of membrane charging in Fig. 5 suggest that a time interval of at least 450–500 ns is required for the formation of an appropriate amount of inactivation-relevant irreversible pores at an external field amplitude of 40 kV/cm.

Irrespective of the exact membrane voltage value required for effective membrane permeabilization, by applying an external field strength of $E = 120$ kV/cm, the membrane segment at the equator of the cell is already charged within about 20 ns to $V_m = 0.5$ V (Fig. 5, middle). In this case, the conditions for membrane permeabilization are already provided shortly after pulse application along the entire membrane surface. The remaining time for pore formation is about 80 ns in case of a pulse 100 ns in duration.

As expected from the above considerations, experiments at higher pulse amplitudes confirm an increase in inactivation efficiency for short pulses (Fig. 6, left). Within a pulse duration range of 100 ns $< T <$ 10 µs, the field amplitude toward shorter pulses was increased up to 125 kV/cm (Fig. 6, middle). When elevating the field strength for 100 and 200 ns pulses to 125 and 120 kV/cm, respectively, an inactivation rate of 3.3 and 3.5 log was obtained. The inactivation rate for longer pulses, 600 ns $< T <$ 10 µs, remained on average at a value comparable to the previously obtained log rates of inactivation obtained for a constant treatment field strength of 40 kV/cm (Fig. 4, left). Again, for this experiment, the treatment energy was fixed to 120 J/ml by an appropriate choice of the number of pulses per treatment. This experiment further illustrates that for a treatment field strength of 120 kV/cm or slightly higher, a time interval of about 80 ns is sufficient to provide membrane permeabilization resulting in the same inactivation rate obtained for 40 kV/cm and 600-ns-long pulses.

The experiments so far indicate that inactivation performance is high if the time required for charging the entire

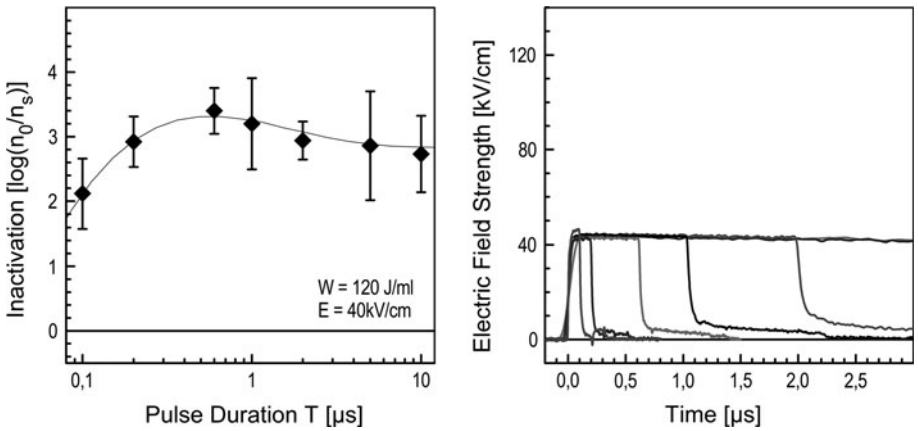

Fig. 4 Inactivation rate over pulse duration at a constant treatment energy value of $W = 120$ J/ml and at an electric field strength of 40 kV/cm. The pulse duration was varied between 100 ns and 10 µs. Inactivation rate decreases for pulses shorter than $T < 600$ ns. For this experiment, three daily independent sets of two samples each were treated

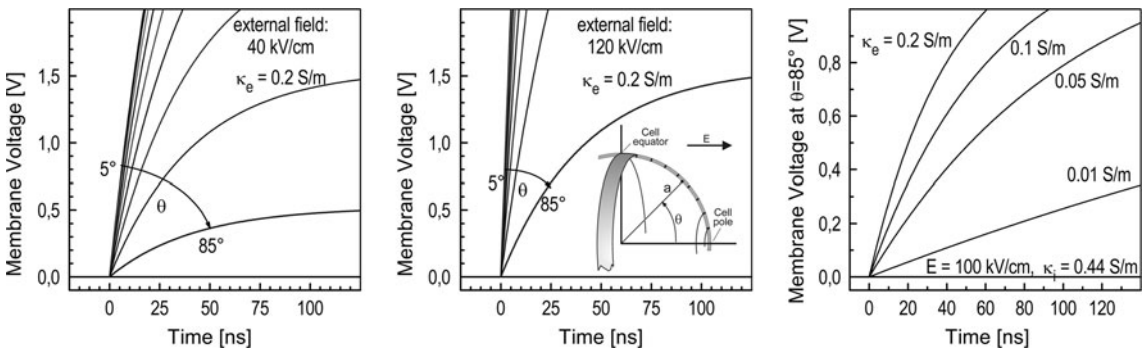

Fig. 5 Calculation of the time course of membrane charging of a spherical cell, $a = 1$ µm at nine different toroidal membrane segments, $\theta_i \pm 5°$, $\theta_i = [5°, 85°, \Delta\theta: 10°]$, for a field amplitude of $E = 40$ kV/cm (*left*), and $E = 120$ kV/cm (*middle*), at an external conductivity of $\kappa_e = 0.2$ S/m. The diagram on the *right* shows the time course of membrane charging at the equatorial membrane segments, $\theta = 85°$, for different conductivities of the extracellular medium and for a pulse amplitude of $E = 100$ kV/cm

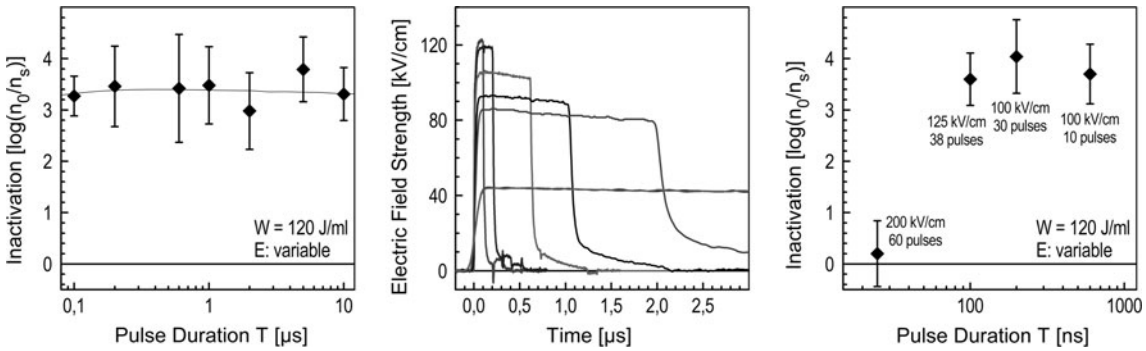

Fig. 6 Inactivation rate over pulse duration for increasing electric field amplitude toward shorter pulses (*middle*). The treatment energy was fixed to $W = 120$ J/ml. The inactivation rate does not depend on pulse amplitude and duration for a pulse duration of 100 ns $> T >$ 10 µs (*left*). Results of an independent experiment for detail analysis within the pulse duration range of 600 ns and less (*right*)

membrane surface to a value of 0.5 V, in particular at equatorial regions, is short compared to the duration of the pulse. For this condition, constant treatment energy delivered to the bacterial suspension results in pulse–duration–invariant inactivation rates within the pulse duration and field value range under consideration in this study. The results further indicate that the energy can be delivered in fractions of various durations. Four pulses of 10 µs and 40 kV/cm and 38 pulses of 100 ns and 125 kV/cm, for example, result in the same inactivation rate. Thus, inactivation of bacteria by successive electric field pulses is suggested to be a cumulative effect. Bacteria obviously cannot recover from PEF exposure within a time of 2 s between two pulses. Within a pulse duration range of 100 ns $> T >$ 10 µs and at invariable suspension conductivity, inactivation does not depend on pulse duration in

cases in which external field amplitude is high enough to provide fast membrane charging at the entire cell surface.

Another independent measurement set, focusing on pulse durations of less than $T \leq 600$ ns, was extended by 25 ns pulses at 200 kV/cm (Fig. 6, right). For 100-ns-long, 200-ns-long, and 600-ns-long pulses, the inactivation rates of the previous set of results (Fig. 6, left) could be confirmed, whereas in case of applying 25-ns-long pulses, no inactivation could be obtained, although the treatment field strength was $E = 200$ kV/cm and the treatment energy also adjusted to $W = 120$ J/ml. According to Eq. (1), in this case the time until the membrane voltage exceeds $V_m = 0.5$ V is about 10 ns at the equatorial segment and a few nanoseconds at the cell poles. In consequence, a period of 15–25 ns is too short for causing inactivation-relevant membrane permeabilization to *P. putida*. This result further proves that intracellular effects, e.g., apoptosis (Engelberg-Kulka et al. 2004, 2006; Hayes 2003), provoked by nanosecond-level PEF, as were reported for mammalian cells treated with comparable parameters (Schoenbach et al. 2004), do not play a major role in bacterial inactivation processes.

For subsequent parameter studies on the basic influence of suspension conductivity, the treatment energy was restricted to 30 J/ml $> W >$ 120 J/ml, which on one hand provides satisfying inactivation performance at the upper limit and on the other hand represents a high-inactivation-gradient working range, ensuring high sensitivity of the inactivation rate to variations of treatment parameter. To exclude a possible influence of insufficient membrane charging on inactivation, the field amplitude was adjusted to high values of 80 kV/cm for 2 µs pulses and 100 kV/cm for 600 ns pulses, respectively.

During the first set of experiments, the number of pulses was fixed to 10 for 600 ns pulses and to five pulses for the 2 µs pulses (Fig. 7, upper row). Although the treatment energy delivered to the suspension considerably decreased, the log rate of inactivation for $0.05 > \kappa_e > 0.2$ S/m remained at a comparable value between 3 and 3.8, which was a typical value obtained for treatments at 120 J/ml and 0.2 S/m so far (cf. Figs. 3, 4, 6). If a pronounced energy dependency of the inactivation rate would exist at field values providing sufficient membrane charging, i.e., $E > 40$ kV/cm and $T > 600$ ns, the inactivation rate should decrease to about 1 log of inactivation for a treatment energy of 30 J/ml (cf. Fig. 3).

At a conductivity of $\kappa_e = 0.01$ S/m, a strong decrease of the inactivation performance was obtained. The log rate of inactivation was 0.5 for 10 pulses and 1.9 for 200 pulses, respectively. This again can be attributed to insufficient membrane charging at the equatorial membrane segments (Fig. 5, left). For a conductivity of the extracellular medium of 0.01 S/m, the membrane voltage at $\theta = 85°$ reaches a value of $V_m = 0.5$ V after 230 ns. Even if the membrane voltage value of $V_m = 0.5$ V in this case is reached during the pulse, the slow character of membrane charging of equatorial segments is comparable to the membrane charging conditions for 100 ns pulses at 40 kV/cm and 0.2 S/m, where rates of only less than 2 log of inactivation could also be obtained.

The second set of experiments was performed at a constant treatment energy of $W = 120$ J/ml. Again, the number of pulses was adjusted for constant energy delivery to the suspension. Here a pronounced increase of inactivation could be obtained for small conductivity values between $0.05 > \kappa_e > 0.2$ S/m (Fig. 7, lower row). As already discussed, at a conductivity of 0.01 S/m, inactivation performance decreases as a result of insufficient membrane charging at the equatorial membrane segments.

Bipolar pulse protocols are proven to be advantageous for PEF processing in general because it decreases electrochemical erosion of treatment electrodes (Kotnik et al. 2001a, b). In this study, inactivation performance was checked for 600 and 1,200 ns bipolar pulses.

For 600 ns bipolar pulses, poor inactivation performance of only 1.1 log of inactivation on average could be obtained. Despite applying equal treatment energy values and field strength conditions, which were efficient previously (i.e., $W = 120$ J/ml and $E = 100$ kV/cm), the inactivation rate was even lower than for 100 ns unipolar pulses (cf. Fig. 4). For short pulse duration of the half waves, the missing time for membrane permeabilization consumed by recharging the membrane to the opposite polarity obviously impairs inactivation-relevant membrane permeabilization and pore growth. The observed decrease in inactivation rate most probably is due to the reduction in time at the high membrane voltage V_m needed for effective membrane permeabilization.

This behavior could not be obtained for 1,200 ns bipolar pulses (Fig. 8). Here, inactivation performance of five bipolar pulses and ten 600 ns unipolar pulses, also representing a treatment energy of $W = 120$ J/ml, was the same and is in good agreement to the experimental results of previous experiments at this energy expenditure. In general, compared to unipolar pulses of the same half-wave duration, the bipolar pulse protocols for bacterial inactivation of *P. putida* do not affect inactivation efficiency.

Large-scale applications of PEF inactivation of bacteria demand simple and reliable pulse generators in the kilojoule range. Spark-gap switched square pulse generation at this energy scale requires pulse-forming network generators, which are elaborate in design and manufacturing compared to Marx-type generators. To decide on appropriate pulse-forming concepts, the inactivation performance of exponential decaying and square pulses was compared to the short-pulse regimen (Fig. 9). In all cases,

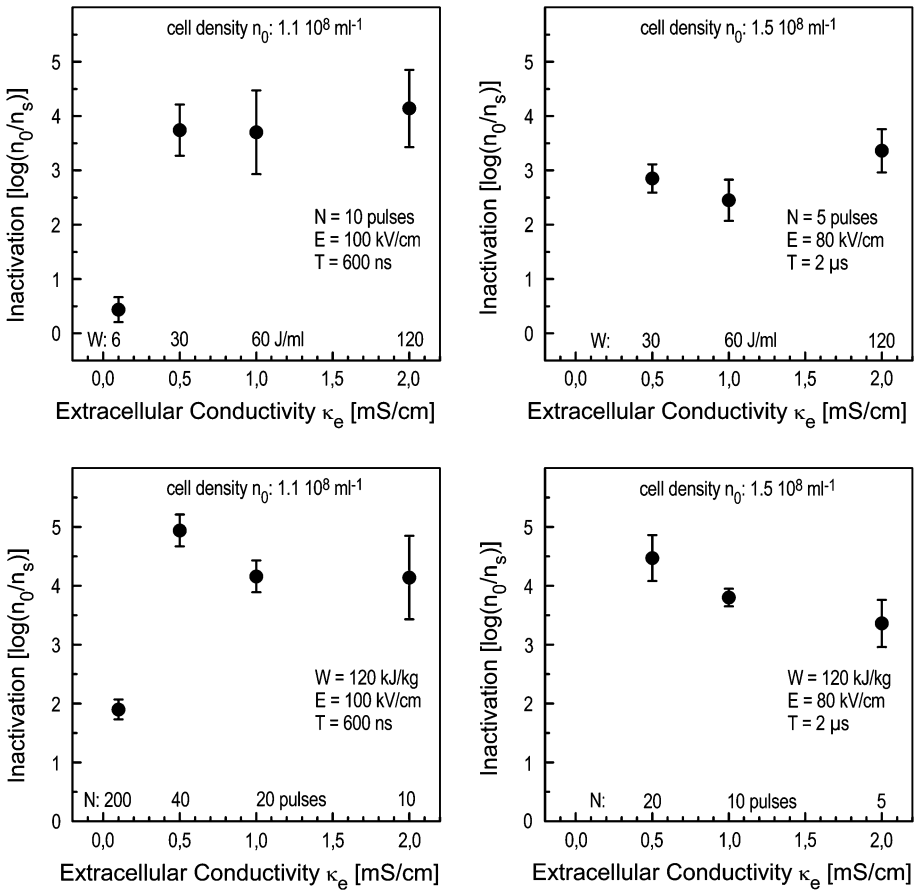

Fig. 7 Influence of extracellular media conductivity on inactivation performance for a constant number of pulses delivered to the suspension (*top row*) and a constant treatment energy (*bottom row*)

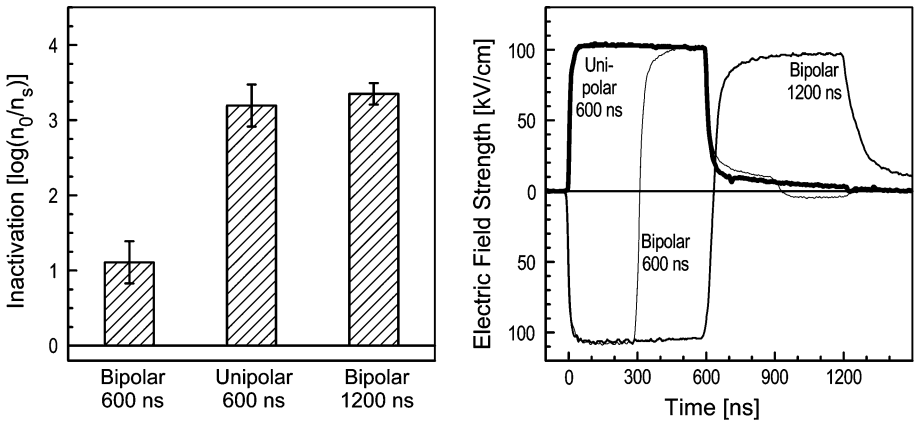

Fig. 8 Inactivation performance of bipolar pulses compared to 600-ns-long unipolar pulses. Extracellular conductivity was $\kappa_e = 0.2$ S/cm

the treatment energy was fixed to $W = 80$ J/ml. Best-inactivation performance of 3.4 log rates of inactivation could be achieved for 600 ns square pulses. Only slightly lower values of 3.25 log of inactivation could be obtained for 160 kV/cm exponential pulses and 2.9 log for 80 kV/cm exponential pulses. In comparison, square pulses realize the best inactivation performance. On this background, for economic reasons in terms of facility investment costs, it might be more advantageous to apply Marx generator concepts, which provide exponential pulses basically by discharging a capacitor bank, instead of pulse-forming networks for square pulse generation, and to compensate for the lower inactivation performance by a higher amount of treatment energy.

Discussion

Our objective was to identify the major impact parameters of PEF inactivation of bacteria and their interaction with regard to inactivation efficiency. The study was performed on *P. putida,* which is a typical Gram-negative

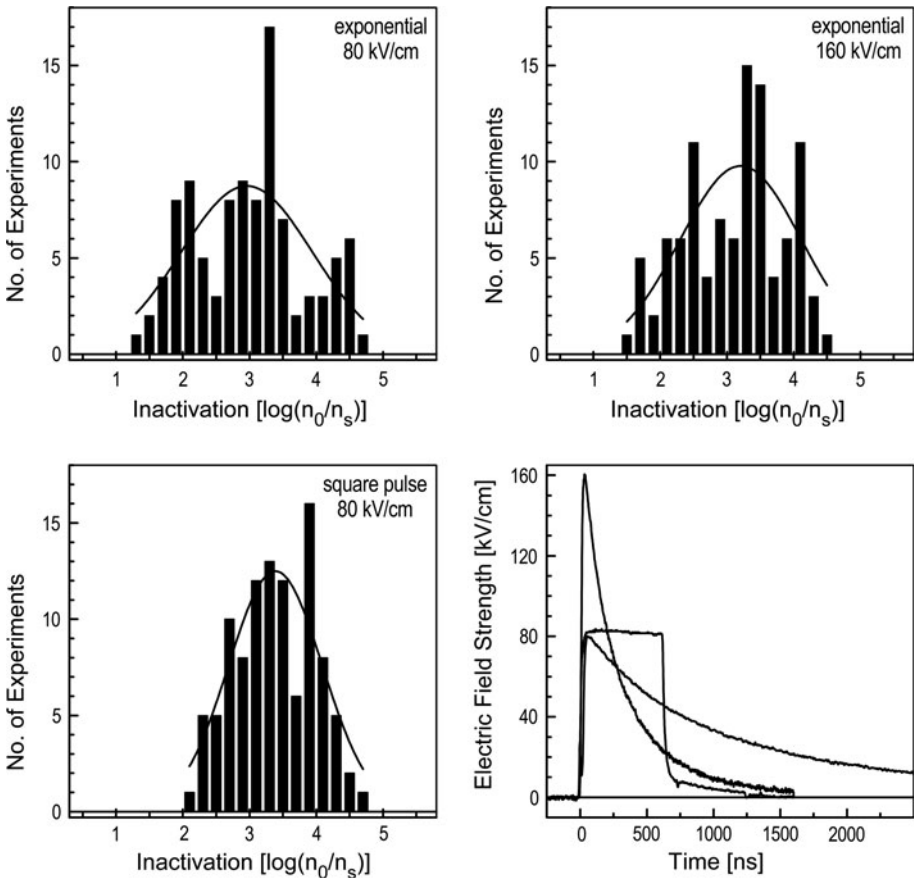

Fig. 9 Comparison of the inactivation performance of square pulses and exponential pulses. The frequency of inactivation values was fitted by a second-order polynomial exponential function. Suspension conductivity was 0.2 S/m. Number of individual experiments was 308

microorganism widely present in the aquatic environment, particularly in wastewater. To isolate the pure effect of electric field processing on inactivation, for all experiments the bacteria suspension was cooled during PEF treatment, thus limiting media temperature rise to less than 7 °C. Because information about media temperature conditions is rare in the literature, absolute values of the log rate of inactivation achieved in this study are hard to compare. Nevertheless, inactivation results on Gram-negative bacteria suspended in buffer media of comparable conductivity, $\kappa_e \sim 0.2$ S/m, and treated at a field strength of more than $E > 20$ kV/cm confirm the order of magnitude of inactivation of 3–4 log rates for a treatment energy of about 150 J/ml, as obtained in this study (Álvarez et al. 2003b; Aronsson et al. 2001; Hülsheger and Niemann 1980; Wouters et al. 2001a). For comparison, treatment energy values in most cases have to be calculated according to Eq. (2), which can only be applied for uniform field distributions in the treatment chamber and for given field strength and treatment time values.

Compared to alternative bacterial inactivation methods, which exhibit a linear dose dependency (Mohamed et al. 2012), e.g., the application γ-irradiation and ultrahigh pressure, PEF inactivation is characterized by a saturation behavior that limits inactivation of *P. putida* to a 6 log reduction at a treatment energy expenditure of $W = 800$ J/ml (Fig. 3). This saturation behavior of PEF inactivation performance at inactivation rate values larger than 3 log also was obtained for *Listeria monocytogenes* exposed to 3 µs bipolar pulses (Mohamed et al. 2012), as well as for *E. coli* (Álvarez et al. 2003b) and *Lactobacillus plantarum* (Abram et al. 2003), all treated with pulses shorter than 5 µs and at a cell density of higher than 3×10^7 cells/ml. It is reported in the literature that the rate of permeabilized cells (Pucihar et al. 2007) as well as the inactivation rate increase with decreasing cell density (Damar et al. 2002; Donsi et al. 2007). At high cell densities, clustering of cells can occur. The cells in the core of a cluster experience lower electric field values (Pucihar et al. 2007), which is supposed to reduce inactivation efficiency at high cell densities. Turbulent mixing of the bacterial suspension, e.g., in continuous flow treatment chambers, was shown to improve inactivation performance considerably (Jaeger et al. 2009; Pataro et al. 2011) by either breaking clusters or by rotating the cell in the field volume (Schrive et al. 2006). To what extent a subpopulation of bacteria possibly exhibiting a high repair mechanism activity might cause the saturation behavior cannot be clarified on the basis of results obtained in this study and needs further investigation. Nevertheless, according to our results, a complete

inactivation of bacteria populations by PEF treatment of suspensions at a cell between 10^7 and 10^8 cells/ml in batch-operation mode and kept at room temperature could not be accomplished. More work is needed to assess the significance of continuous-flow treatment concepts and of synergies between PEF treatment and other methods of microbial decontamination, e.g., thermal heating (Alkhafaji and Farid 2007; Saldana et al. 2011; Sepulveda et al. 2005; Toepfl et al. 2007), for increasing inactivation efficiency.

Concerning pulse parameter optimization for energy-efficient PEF inactivation of microorganisms, the entire cell membrane has to be rapidly charged to values above $V_m > 0.5$ V, which represents a necessary condition for the onset of inactivation-relevant pore formation. After reaching this value, the remaining time during the pulse for pore formation and growth has to be 80 ns for a pulse amplitude of 120 kV/cm (cf. Fig. 5, middle, and Fig. 6), and about 500 ns for 40 kV/cm (cf. Fig. 5, left, and Fig. 4), at minimum. When providing a sufficiently high membrane voltage and pore formation time over the entire bacterial surface, the log rate of inactivation for a given extracellular conductivity does not depend on pulse duration within 100 ns $> T >$ 10 µs, but only on overall treatment time $N{\cdot}T$ and field amplitude E, which represents a pure treatment energy dependency at a given conductivity value. For fixed energy delivered to the bacterial suspension, the log rate of inactivation remains at a constant value (Fig. 6). In case of shorter pulses, $T = 25$ ns, even if the treatment field strength is adjusted to 200 kV/cm and $V_m > 0.5$ V at the equatorial membrane segment is reached within 10 ns at the latest, inactivation performance at the same value of expended energy of 120 J/ml is almost zero (Fig. 6, right). From this experiment, it can be concluded that a time interval of about 15–20 ns is too short for the generation of inactivation-relevant pores and that intracellular effects, e.g., apoptosis (Engelberg-Kulka et al. 2006; Hayes 2003; Schoenbach et al. 2004), do not play an important role in bacterial inactivation. The fact that bacteria could not be inactivated by applying nanosecond-level pulses is in agreement with the findings of recent experiments (Zgalin et al. 2012).

At this point it should be mentioned that for the calculation of the dynamics of membrane charging, the cell was considered to be spherical for reasons of simplicity. However, *P. putida* exhibits an elliptical rod-type shape with a minor axis radius of 0.5 µm and a major axis radius of about 2 µm. Compared to spherical cells with a radius of $a = 1$ µm, this results in a higher membrane voltage at the cell poles in case the long axis of the bacterium is oriented parallel to the direction of the electric field, but also in smaller values at the critical equatorial cell segments (Kotnik et al. 1998, 2010). If the field direction is parallel to the minor axis of the ellipsoid, membrane voltage values at the cell poles are smaller as a result of the smaller lateral dimension, but also the surface fraction of equatorial segments exhibiting poor membrane charging is smaller. In case a normal angular distribution of the orientation angle of the bacteria's major axis with respect to the field direction within a large bacteria collective is assumed, it appears feasible for the high electric fields used in this study that deteriorated permeabilization conditions along surface regions of elliptically shaped cells are compensated by improved conditions at other surface regions along the same cell, all in all resulting in comparable inactivation-relevant membrane permeabilization as estimated by considerations on a spherical model. Nevertheless, a clarification of this point cannot be accomplished by the approaches we used here. Despite these limitations, our results reveal a satisfying correlation between high inactivation performance and fast membrane charging to 0.5 V, even when applying a simple spherical cell model.

The statement that the log rate of inactivation does not change with square pulse duration for a fixed suspension conductivity and treatment energy can be extended to alternative pulse shapes. Bipolar pulses were found to be as effective as square pulses if the half-wave duration is long enough for fast entire-membrane-surface charging (Fig. 8). A particular high inactivation efficiency of bipolar pulse protocols of 7 log of inactivation (Ho et al. 1995) could not be confirmed for bipolar pulses of 300 and 600 ns half-wave duration for *P. putida*. Furthermore, exponential pulses of 80 and 160 kV/cm and exhibiting an energy content comparable to 600 ns, 80 kV/cm square pulses, were found to be almost as effective as square pulses. In the most unfavorable case of low-amplitude exponential pulses, the inactivation rate was only reduced by 0.5 log (Fig. 9). This reduction in inactivation performance demanding slightly higher treatment energy expenditures might be compensated by lower investment costs of Marx-type pulse generators compared to pulse-forming network concepts required for square pulse generation.

All the above refers to PEF inactivation performance at a constant suspension conductivity of $\kappa_e = 0.2$ S/m. When extracellular conductivity was decreased, comparable values of log reduction of inactivation could only be obtained for similar overall treatment durations, i.e., the product of number of pulses and pulse duration $N{\cdot}T$ (Fig. 7, upper row). In comparison, treatment protocols delivering the same energy to the suspensions of different conductivity resulted in distinct higher inactivation rates at low buffer conductivities (Fig. 7, lower row). At very low conductivities, $\kappa_e = 0.01$ S/m, again, insufficient membrane charging at the equatorial cell segments impairs inactivation performance (Fig. 5, right). PEF inactivation of low-conductivity suspensions is thus not efficient in cases of application of submicrosecond pulses (Katsuki et al. 2002).

In summary, for efficient PEF inactivation of bacteria, pulse amplitude and duration have to be chosen for fast entire-membrane surface charging. Membrane charging can be estimated on the first order by the Pauly and Schwan (1959) model. Critical surface elements with respect to sufficient charging are equatorial ring segments. Given optimum membrane charging conditions, i.e., appropriate high field amplitude and pulses long enough for pore formation, the inactivation rate is dominated by the overall treatment time within a range of suspension conductivity of $0.05 > \kappa_e > 0.2$ S/m. For a fixed extracellular conductivity, comparable inactivation rates can be achieved by constant treatment energy expenditure. For short-pulse PEF inactivation, the pulse shape plays a minor part and can be chosen for generator concept preference in case pulse amplitude is high enough for fast entire-surface membrane charging.

Acknowledgments The authors acknowledge the efforts of Silke Kirchen and Silke-Mareike Marten for CFU analysis; the help of Rüdiger Wüstner in preparing and performing the pulse experiments; and the detailed discussions of Aude Silve on membrane charging. The authors appreciate the helpful scientific discussions on bacterial inactivation within the framework of COST TD1104. This study was funded by BMBF grant 02WT0675, administered by the Karlsruhe Institute of Technology.

References

Abram F, Smelt JPPM, Bos R, Wouters PC (2003) Modelling and optimization of inactivation of *Lactobacillus plantarum* by pulsed electric field treatment. J Appl Microbiol 94:571–579

Ait-Ouazzou A, Espina L, García-Gonzalo D, Pagán R (2013) Synergistic combination of physical treatments and carvacrol for *Escherichia coli* O157:H7 inactivation in apple, mango, orange, and tomato juices. Food Control 161:23–30

Alkhafaji SR, Farid M (2007) An investigation on pulsed electric fields technology using new treatment chamber design. Innov Food Sci Emerg Technol 8:205–212

Álvarez I, Pagán R, Condón S, Raso J (2003a) The influence of process parameters for the inactivation of *Listeria monocytogenes* by pulsed electric fields. Int J Food Microbiol 87:87–95

Álvarez I, Virto R, Raso J, Condón S (2003b) Comparing predicting models for the *Escherichia coli* inactivation by pulsed electric fields. Innov Food Sci Emerg Technol 4:195–202

Aronsson K, Lindgren M, Johansson BR, Rönner U (2001) Inactivation of microorganisms using pulsed electric fields: the influence of process parameters on *Escherichia coli*, *Listeria innocua*, *Leuconostoc mesenteroides* and *Saccharomyces cerevisiae*. Innov Food Sci Emerg Technol 2:41–54

Castro AJ, Barbosa-Canovas GV, Swanson BG (1993) Microbial inactivation of foods by pulsed electric fields. J Food Proc Preserv 17:47–73

Damar S, Bozoglu F, Hizal M, Bayindirli A (2002) Inactivation and injury of *Escherichia coli* O157:H7 and *Staphylococcus aureus* by pulsed electric fields. World J Microbiol Biotechnol 18:1–6

Donsi G, Ferrari G, Pataro G (2007) Inactivation kinetics of *Saccharomyces cerevisiae* by pulsed electric fields in a batch treatment chamber: the effect of electric field unevenness and initial cell concentration. J Food Eng 78:784–792

Eing CJ, Bonnet S, Pacher M, Puchta H, Frey W (2009) Effects of nanosecond pulsed electric field exposure on *Arabidopsis thaliana*. IEEE Trans Dielectr Electr Insul 16:1322–1328

Engelberg-Kulka H, Sat B, Reches M, Amitai S, Hazan R (2004) Bacterial programmed cell death systems as targets for antibiotics. Trends Microbiol 12:66–71

Engelberg-Kulka H, Amitai S, Kolodkin-Gal I, Hazan R (2006) Bacterial programmed cell death and multicellular behavior in bacteria. PLoS Genet 2:e135

Flickinger B, Berghofer T, Hohenberger P, Eing C, Frey W (2010) Transmembrane potential measurements on plant cells using the voltage-sensitive dye ANNINE-6. Protoplasma 247:3–12

Frey W, White JA, Price RO, Blackmore PF, Joshi RP, Nuccitelli R, Beebe SJ, Schoenbach KH, Kolb JF (2006) Plasma membrane voltage changes during nanosecond pulsed electric field exposure. Biophys J 90:3608–3615

Frey W, Sack M, Wuestner R, Mueller G (2009) Gas-insulated self-breakdown spark gaps: aspects on low-scattering and long-lifetime switching. Acta Phys Pol A 115:1016–1018

Gabriel B, Teissié J (1997) Direct observation in the millisecond time range of fluorescent molecule asymmetrical interaction with the electropermeabilized cell membrane. Biophys J 73:2630–2637

Galapate RP, Baes AU, Okada M (2001) Transformation of dissolved organic matter during ozonation: effects on trihalomethane formation potential. Water Res 35:2201–2206

Garcia D, Gomez N, Condon S, Raso J, Pagan R (2003) Pulsed electric fields cause sublethal injury in *Escherichia coli*. Lett Appl Microbiol 36:140–144

Gusbeth C, Frey W, Volkmann H, Schwartz T, Bluhm H (2009) Pulsed electric field treatment for bacteria reduction and its impact on hospital wastewater. Chemosphere 75:228–233

Hamilton WA, Sale AJH (1967) Effects of high electric fields on microorganisms: II. Mechanism of action of the lethal effect. Biochim Biophys Acta 148:789–800

Hayes F (2003) Toxins–antitoxins: plasmid maintenance, programmed cell death, and cell cycle arrest. Science 301:1496–1499

Heinz V, Sitzmann W, Töpfl S (2007) Selektive Abtötung von zellulären Krankheitserregern und Verderbsorganismen: Das ELSTERIL®-Verfahren. Chem Eng Technol 79:1135–1143

Hibino M, Itoh H, Kinosita K Jr (1993) Time courses of cell electroporation as revealed by submicrosecond imaging of transmembrane potential. Biophys J 64:1789–1800

Ho SY, Mittal GS, Cross JD, Griffiths MW (1995) Inactivation of *Pseudomonas fluorescens* by high voltage electric pulses. J Food Sci 60:1337

Hoelzel R (1999) Non-invasive determination of bacterial single cell properties by electrorotation. Biochim Biophys Acta Mol Cell Res 1450:53–60

Huang KC, Mukhopadhyay R, Wen BN, Gitai Z, Wingreen NS (2008) Cell shape and cell-wall organization in gram-negative bacteria. Proc Natl Acad Sci U S A 105:19282–19287

Huang K, Tian H, Gai L, Wang J (2012) A review of kinetic models for inactivating microorganisms and enzymes by pulsed electric field processing. J Food Eng 111:191–207

Hülsheger H, Niemann EG (1980) Lethal effects of high-voltage pulses on *E. coli* K12. Radiat Environ Biophys 18:281–288

Hülsheger H, Potel J, Niemann EG (1981) Killing of bacteria with electric pulses of high field strength. Radiat Environ Biophys 20:53–65

Jaeger H, Meneses N, Knorr D (2009) Impact of PEF treatment inhomogeneity such as electric field distribution, flow characteristics and temperature effects on the inactivation of *E. coli* and milk alkaline phosphatase. Innov Food Sci Emerg Technol 10:470–480

Jungfer C, Schwartz T, Obst U (2007) UV-induced dark repair mechanisms in bacteria associated with drinking water. Water Res 41:188–196

Katsuki S, Moreira K, Dobbs F, Joshi RP, Schoenbach KH (2002) Bacterial decontamination with nanosecond pulsed electric fields. In: Power Modulator Symposium, 2002 and 2002 High-Voltage Workshop, Record of the Twenty-Fifth International Conference, pp 648–651

Kotnik T, Miklavcic D, Slivnik T (1998) Time course of transmembrane voltage induced by time-varying electric fields—a method for theoretical analysis and its application. Bioelectrochem Bioenerg 45:3–16

Kotnik T, Miklavčič D, Mir LM (2001a) Cell membrane electropermeabilization by symmetrical bipolar rectangular pulses: part II. Reduced electrolytic contamination. Bioelectrochemistry 54:91–95

Kotnik T, Mir LM, Flisar K, Puc M, Miklavčič D (2001b) Cell membrane electropermeabilization by symmetrical bipolar rectangular pulses: part I. Increased efficiency of permeabilization. Bioelectrochemistry 54:83–90

Kotnik T, Pucihar G, Miklavcic D (2010) Induced transmembrane voltage and its correlation with electroporation-mediated molecular transport. J Membr Biol 236:3–13

Mohamed HMH, Diono BHS, Yousef AE (2012) Structural changes in *Listeria monocytogenes* treated with gamma radiation pulsed electric field and ultra-high pressure. J Food Saf 32:66–73

Neu JC, Krassowska W (1999) Asymptotic model of electroporation. Phys Rev E 59:3471–3482

Neumann E, Sowers AE, Jordan CA (1989) Electroporation and electrofusion in cell biology. Plenum, New York

Nystrom T (2004) Stationary-phase physiology. Annu Rev Microbiol 58:161–181

Pataro G, Senatore B, Donsi G, Ferrari G (2011) Effect of electric and flow parameters on PEF treatment efficiency. J Food Eng 105:79–88

Pauly H, Schwan HP (1959) Uber Die Impedanz Einer Suspension Von Kugelformigen Teilchen Mit Einer Schale—Ein Modell Fur Das Dielektrische Verhalten Von Zellsuspensionen Und Von Proteinlosungen. Zeitschrift Fur Naturforschung Part B—Chemie Biochemie Biophysik Biologie Und Verwandten Gebiete 14:125–131

Poyatos JM, Almecija MC, Garcia-Mesa JJ, Munio MM, Hontoria E, Torres JC, Osorio F (2011) Advanced methods for the elimination of microorganisms in industrial treatments: potential applicability to wastewater reuse. Water Environ Res 83:233–246

Pucihar G, Kotnik T, Teissié J, Miklavcic D (2007) Electropermeabilization of dense cell suspensions. Eur Biophys J Biophys Lett 36:173–185

Reasoner DJ, Geldreich EE (1985) A new medium for the enumeration and subculture of bacteria from potable water. Appl Environ Microbiol 49:1–7

Rieder A, Schwartz T, Schon-Holz K, Marten SM, Suss J, Gusbeth C, Kohnen W, Swoboda W, Obst U, Frey W (2008) Molecular monitoring of inactivation efficiencies of bacteria during pulsed electric field treatment of clinical wastewater. J Appl Microbiol 105:2035–2045

Sakarauchi Y, Kondo E (1980) Lethal effects of high electric fields on microorganisms. J Agric Chem Soc Jpn 54:837–844

Saldana G, Puertolas E, Monfort S, Raso J, Alvarez I (2011) Defining treatment conditions for pulsed electric field pasteurization of apple juice. Int J Food Microbiol 151:29–35

Sale AJH, Hamilton WA (1967) Effects of high electric fields on microorganisms: I. Killing of bacteria and yeasts. Biochim Biophys Acta 148:781–788

Sale AJH, Hamilton WA (1968) Effects of high electric fields on micro-organisms: III. Lysis of erythrocytes and protoplasts. Biochim Biophys Acta Biomembr 163:37–43

Saulis G (2010) Electroporation of cell membranes: the fundamental effects of pulsed electric fields in food processing. Food Eng Rev 2:52–73

Schoenbach KH, Joshi RP, Stark RH, Dobbs FC, Beebe SJ (2000) Bacterial decontamination of liquids with pulsed electric fields. IEEE Trans Dielectr Electr Insul 7:637–645

Schoenbach KH, Joshi RP, Kolb JF, Chen NY, Stacey M, Blackmore PF, Buescher ES, Beebe SJ (2004) Ultrashort electrical pulses open a new gateway into biological cells. Proc IEEE 92:1122–1137

Schoenbach KH, Joshi RP, Beebe SJ, Baum CE (2009) A scaling law for membrane permeabilization with nanopulses. IEEE Trans Dielectr Electr Insul 16:1224–1235

Schrive L, Grasmick A, Moussiere S, Sarrade S (2006) Pulsed electric field treatment of *Saccharomyces cerevisiae* suspensions: a mechanistic approach coupling energy transfer, mass transfer and hydrodynamics. Biochem Eng J 27:212–224

Sepulveda DR, Gongora-Nieto MM, San-Martin MF, Barbosa-Canovas GV (2005) Influence of treatment temperature on the inactivation of Listeria innocua by pulsed electric fields. LWT Food Sci Technol 38:167–172

Silhavy TJ, Kahne D, Walker S (2010) The bacterial cell envelope. Cold Spring Harb Perspect Biol 2:a000414

Smith PW (2002) Transient electronics: pulsed circuit technology. Wiley, Chichester

Sobrino-López A, Martín-Belloso O (2010) Potential of high-intensity pulsed electric field technology for milk processing. Review. Food Eng Rev 2:17–27

Sohn J, Amy G, Cho J, Lee Y, Yoon Y (2004) Disinfectant decay and disinfection by-products formation model development: chlorination and ozonation by-products. Water Res 38:2461–2478

Teissié J, Rols MP (1993) An experimental evaluation of the critical potential difference inducing cell membrane electropermeabilization. Biophys J 65:409–413

Teissié J, Golzio M, Rols MP (2005) Mechanisms of cell membrane electropermeabilization: a minireview of our present (lack of?) knowledge. Biochim Biophys Acta 1724:270–280

Toepfl S, Heinz V, Knorr D (2007) High intensity pulsed electric fields applied for food preservation. Chem Eng Proc Process Intensif 46:537–546

Tsong TY (1990) On electroporation of cell-membranes and some related phenomena. Bioelectrochem Bioenerg 24:271–295

Vasilkoski Z, Esser AT, Gowrishankar TR, Weaver JC (2006) Membrane electroporation: the absolute rate equation and nanosecond time scale pore creation. Phys Rev E 74:21904-1–21904-12

Weaver JC, Chizmadzhev YA (1996) Theory of electroporation: a review. Bioelectrochem Bioenerg 41:135–160

Weaver JC, Smith KC, Esser AT, Son RS, Gowrishankar TR (2012) A brief overview of electroporation pulse strength-duration space: a region where additional intracellular effects are expected. Bioelectrochemistry 87:236–243

Wouters PC, Alvarez I, Raso J (2001a) Critical factors determining inactivation kinetics by pulsed electric field food processing. Trends Food Sci Technol 12:112–121

Wouters PC, Bos AP, Ueckert J (2001b) Membrane permeabilization in relation to inactivation kinetics of Lactobacillus species due to pulsed electric fields. Appl Environ Microbiol 67:3092–3101

Zgalin MK, Hodzic D, Rebersek M, Kanduser M (2012) Combination of microsecond and nanosecond pulsed electric field treatments for inactivation of *Escherichia coli* in water samples. J Membr Biol 245:643–650

Zimmermann U, Pilwat G, Riemann F (1974) Dielectric-breakdown of cell-membranes. Biophys J 14:881–899